

# Synthesis and Characterization of Hollow and Non-Hollow Monodisperse Colloidal TiO<sub>2</sub> Particles

S. Eiden-Assmann,\* J. Widoniak, and G. Maret

Fachbereich Physik, Universität Konstanz, Konstanz, Germany

## ABSTRACT

Monodisperse spherical hollow and non hollow titania particles of variable sizes are produced in a sol gel synthesis from Ti(EtO)<sub>4</sub> in ethanol. Hollow spherical particles of rutile were obtained by coating colloidal polystyrene beads with a titanium oxide hydrate layer and subsequently calcination at elevated temperatures in oxygen atmosphere. The non hollow titania particles were produced in the presence of salt or polymer solution. The influence of different salt ions or polymer molecules on the size and on the size distribution of the non hollow particles was investigated. Nitrogen absorption measurements revealed that the addition of polymers yields porous titania colloids.

*Key Words:* Sol gel synthesis; Titania particles; N MAS NMR; Powder x ray diffraction; Porosity.

## INTRODUCTION

The production of particles with a specific size and morphology is of primary importance for the development of new materials. Mesoscale spheres of ceramic materials are of particular interest for fundamental research, in order to interpret physical properties or surface interactions quantitatively as a function of the morphology and size of the spheres. Recently, the importance of tailored particles has been recognized in a number of applications such as ceramics,

catalysts, solar cells,<sup>[1]</sup> pigments, and photonic crystals.<sup>[2]</sup>

Hollow particles represent a special case, since they can be used because of their lower density and particular optical properties as extremely small containers and as fillers or pigments.<sup>[3]</sup> For optical applications, hollow and non-hollow titania particles are particularly interesting due to their high refractive index.

Because of their technological importance, different approaches<sup>[4-9]</sup> have been developed. One established method is the precipitation of titania particles from

---

\*Correspondence: S. Eiden Assmann, Fachbereich Physik, Universität Konstanz, 78457 Konstanz, Germany; E mail: stefanie.eiden@uni knostanz.de.

titania alkoxides in aqueous alcohol solution. The method originally reported by Barringer and Bowen<sup>[7]</sup> was found difficult to reproduce and aggregates containing a few spherical colloidal particles were frequently obtained. In previous studies,<sup>[10,11]</sup> the origins of this morphology were investigated and found to result from an interplay of electrostatic, van der Waals, and short range repulsive interaction potentials. If the particle surface potential is raised to a sufficient level, the repulsive interactions are strong enough to prevent Brownian aggregation and uniform particles are formed. Therefore, one method of controlling the stability of the particles is to increase the charge of the particle surface by adding a salt. In the case of titania, Look and Zukoski<sup>[9]</sup> added NaCl or HCl to the precipitation medium and obtained particles with diameters between 800 and 1200 nm, depending on the salt concentration. A second method of controlling the stability of particles is based on the steric stabilization of the particles. Jean and Ring<sup>[6]</sup> used a polymeric stabilization agent, hydroxypropylcellulose, in order to control the size of the colloids. They obtained particles with diameters in a range between 700 and 1200 nm. In order to investigate the influence of steric and electrostatic stabilization on the formation mechanism, the size, and the size distribution of titania particles in more detail, we varied the ionic strength and the type of the stabilizing polymer in the reaction solution.

Here, we describe a simple and reproducible synthesis of well-defined hydrous titania particles that were obtained by adding salt or polymer to the reaction solution. Besides, we report their characterization by electron microscopy, thermogravimetry (TG), <sup>1</sup>H-MAS-NMR, x-ray absorption spectroscopy, nitrogen absorption, and electrophoretic mobility measurements and discuss mechanism of particle formation.

For hollow titania particles, two approaches for coating the polymer beads with a thin TiO<sub>2</sub> shell have been reported. In the first method<sup>[12]</sup> the hollow TiO<sub>2</sub> spheres were produced by coating crystalline arrays of monodisperse polystyrene beads in the sol gel precursor solution. The second approach<sup>[13]</sup> relied on a double-template method. In this method, a colloid crystal of silica beads is formed using a convective assembly process. These crystals were used as template to form a macroporous polymer. After removal of the silica beads, the surface of the macroporous polymer was coated with TiO<sub>2</sub>. Both methods have been successfully applied for the formation of hollow TiO<sub>2</sub> spheres. Nevertheless, the structure of the TiO<sub>2</sub> of the materials was amorphous. Here we describe the successful synthesis of TiO<sub>2</sub> hollow spheres consisting exclusively of crystalline rutile.

## EXPERIMENTAL

### Synthesis

#### Non-Hollow Titania Particles

Monodisperse spherical TiO<sub>2</sub> particles were prepared by controlled hydrolysis of titanium tetraethoxide in ethanol.<sup>[7]</sup> An ethanol volume of 100 mL was mixed with 0.4–0.6 mL of a 0.1 M aqueous salt or polymer solution, followed by addition of 1.5–1.7 mL titanium tetraethoxide at ambient temperature under inert gas atmosphere, using a magnetic stirrer. Reagents must be mixed completely so that nucleation occurs uniformly throughout the solution. Depending on the concentration, visible particle formation started after several seconds or minutes and gave a uniform suspension of TiO<sub>2</sub> beads. After a few minutes, stirring was discontinued. After a few hours the reactions were finished and the spheres were collected on a 200-nm-Millipore filter and washed with ethanol.

#### Hollow Titania Particles

Negatively charged sulfate-stabilized polystyrene beads were prepared as described by Furusawa et al.<sup>[14]</sup> They were coated in a sol gel process with Ti(OEt)<sub>4</sub>. Therefore, the polystyrene beads were dispersed in absolute ethanol by sonication. Subsequently, Ti(OEt)<sub>4</sub> was rapidly added and the dispersion was stirred for 30 min in a closed PE bottle. Finally, the bottle was opened and the sol gel precursor hydrolyzed into the oxide ceramic gel as a result of its exposure to the moisture of the ambient air. After further 24 hr of stirring under ambient atmosphere part of the solvent was evaporated. A homogeneous dense thin coat around each polystyrene bead was formed. The beads were filtered and washed with distilled water. Polystyrene free TiO<sub>2</sub> hollow spheres were obtained by the calcination in oxygen.

### Methods of Characterization

The water content of the TiO<sub>2</sub> beads was determined thermogravimetrically using a Netzsch-thermoanalyzer STA 429 (O<sub>2</sub> atmosphere, heating rate 10 K/min) combining TG, differential thermogravimetry (DTG), and differential thermal analysis (DTA).

The crystallinity and phase-purity of the products were monitored by powder x-ray diffraction (XRD) using a Guinier-Huber camera 600 with CuK<sub>V1</sub> radiation. Scanning electron micrographs (SEM) were obtained on a Philips raster electron microscope (XL Series).

Electrophoretic mobility was measured on a Zetasizer (Brookhaven). Particle mobilities were determined by centrifuging particles out of suspension and resuspending a small fraction of particle sediment in the supernatant for use in mobility determinations.

$^1\text{H}$ -MAS-NMR spectra of  $\text{TiO}_2$  particles, dried at  $100^\circ\text{C}$ , were recorded on a Bruker MSL-400 spectrometer at 400.13 MHz resonance frequency with pulse repetition of 120 sec, pulse width of 2  $\mu\text{sec}$  and a spinning speed of 10.0 kHz.

Nitrogen absorption isotherms were measured at 77 K on a Quantachrome Nova 3000. The samples were outgassed at 475 K and 1 mPa for 12 hr.

X-ray absorption spectroscopic measurements of titania colloids were carried out at station E4 of HASYLAB (DESY, Hamburg). The Ti K-edge EXAFS spectra were obtained in transmission mode under the ring operation conditions of 1.998 GeV and 140 230 mA. The data were analyzed with the program WinXAS 2.2, developed by Ressler.

## RESULTS AND DISCUSSION

### Non-Hollow Titania Particles

#### The Addition of Salt

The concentration of all reactants were varied. A 100 mL ethanol, 1.50 mL  $\text{Ti}(\text{OC}_2\text{H}_5)_4$ , and 0.40 mL of 0.1 M aqueous salt or polymer solution were found to be optimal. Variations in the concentration of ethanol, water, or  $\text{Ti}(\text{OC}_2\text{H}_5)_4$  show no significant effect on the size of the particles, but on the size distribution. Moreover, the size and the size distribution are very sensitive to the type of salt that is added (Table 1). The SEM, [cf. Fig. 1(a)] illustrate that perfectly uniform spherical  $\text{TiO}_2$  colloids are obtained by addition of salts such as alkali halides, and nitrates. With alkali halides, we observe that the particle size decreases with increasing ionic strength in the reaction solution. Beads with diameters of about 2500 nm were obtained with lithium chloride, whereas the use of cesium chloride yielded 200 nm particles. No size changes were obtained when the halide anions were changed; approximately the same results were obtained for alkali bromides and iodides. The electrophoresis results (Table 1) show that an increased positive zeta potential leads to a reduction in particle size. This is correlated, at least with particles formed with KCl, with the ionic strength in the reaction medium. With very high ionic strength no formation of particles was observed. Probably, in this case the ions bind most of the water molecules in the hydration shell, so that not enough water molecules exit for the generation of

**Table 1.** Size and zeta potential of titania particles depending on the addition of different salt solution under following conditions: reaction time, 150 min; 100 mL EtOH; 1.50 mL  $\text{Ti}(\text{OEt})_4$ ; 0.50 mL salt solution.

Salt	Concentration of salt in the reaction solution (M)	Size (nm)	Zeta potential (mV)
LiCl	$4 \times 10^{-4}$	700 2500	9
NaCl	$4 \times 10^{-4}$	$800 \pm 7\%$	16
KCl	$2 \times 10^{-4}$	500 900	20
KCl	$4 \times 10^{-4}$	$300 \pm 5\%$	22
KCl	$8 \times 10^{-4}$	$50 \pm 20\%$	27
KCl	$16 \times 10^{-4}$	No particles	
CsCl	$4 \times 10^{-4}$	$200 \pm 20\%$	25
$\text{KNO}_3$	$4 \times 10^{-4}$	$300 \pm 18\%$	

titania. For different cations, the zeta potential (and hence the degree of cation absorption) increase significant with increasing cation radii. As judged from EDX measurements that show no indications of any salt ions, the cations are not built into the particles.

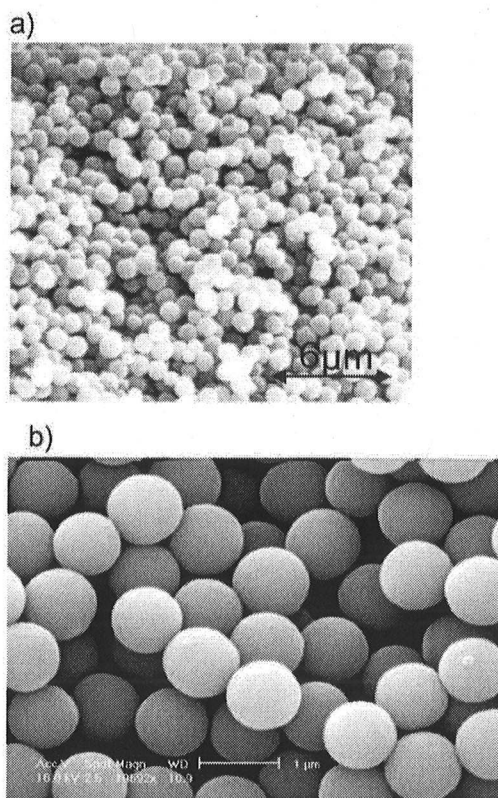


**Figure 1.** (a) SEM picture of the titania particles synthesized by addition of salt, (b) by addition of Lutensol ON 50.

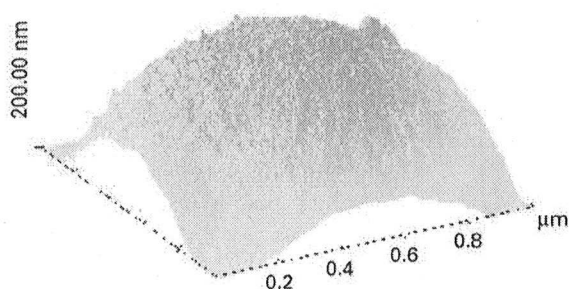


**Figure 2.** AFM picture of a titania particle prepared with sodium chloride. (View this art in color at [www.dekker.com](http://www.dekker.com).)

Bogush and Zukoski likewise reported that changes in the ionic strength affect the formation of titania particles. Bogush et al.<sup>[15,16]</sup> established the growth of the particles is best described, rather than by the LaMer model,<sup>[17]</sup> by an aggregation mechanism that implies that the colloidal particles are formed by the aggregation of small particles with a size of about 5–20 nm (primary particles). They suggested, furthermore, that the formation of primary particles proceeds independently of the existing particles and that the absolute size of the final particles is determined by the size and the aggregation tendencies of the primary particles.

The electrophoresis results show that with increasing stability of the primary particles the size of the

final particles decrease. The effect of the size of the primary particles on the formation of the final particles is difficult to determine. Since the as-synthesized titania particles are amorphous, the size of the primary particles is difficult to determine. The AFM picture shown in Fig. 2 demonstrates that the surface of the final particles is rough. The height variation amounts to about 5 nm. This result indicates that the final particles consist of primary particles with a diameter of about 10 nm.

#### Addition of Polymer

The influence of polymers (Table 2) on the size and size distribution of the colloidal particles was investigated next. Two different types of polymers, diblock-copolymers Lutensol ( $\text{RO}(\text{CH}_2\text{CH}_2\text{O})_x\text{H}$ ) and triblock-copolymers Pluronic ( $\text{PEO}_n\text{PPO}_m\text{PEO}_n$ ), were used for steric stabilization, since the polymers can be assumed to stabilize the primary particles in different ways (Fig. 3), the hydrophilic part of Lutensol is likely to interact with the nanoparticle surface while the hydrophobic part extends into the medium, thus providing additional steric stabilization. In case of Pluronic, the presence of two hydrophilic parts can be assumed to lead a coating of the nanoparticle surfaces. As shown in Fig. 1(b), highly monodisperse particles are obtained in the presence of Lutensol polymer. The size of the

**Table 2.** Size of titania particles depending on the addition of different polymer solution under following conditions: reaction time, 150 min; 100 mL EtOH; 1.50 mL  $\text{Ti}(\text{OEt})_4$ ; 0.50 mL of 0.1 M polymer solution.

Polymer	Formula	Particle size (nm)
Lutensol AO 5	$\text{RO}(\text{CH}_2\text{CH}_2\text{O})_5\text{H}$ R = $\text{C}_{13}\text{C}_{15}$ , oxoalcohol	$800 \pm 3\%$
Lutensol TO 3	$\text{RO}(\text{CH}_2\text{CH}_2\text{O})_3\text{H}$ R = $i\text{C}_{13}\text{H}_{27}$ , oxoalcohol	$800 \pm 3\%$
Lutensol TO 5	$\text{RO}(\text{CH}_2\text{CH}_2\text{O})_5\text{H}$ R = $i\text{C}_{13}\text{H}_{27}$ , oxoalcohol	$800 \pm 3\%$
Lutensol TO 7	$\text{RO}(\text{CH}_2\text{CH}_2\text{O})_7\text{H}$ R = $i\text{C}_{13}\text{H}_{27}$ , oxoalcohol	$800 \pm 3\%$
Lutensol ON 50	$\text{RO}(\text{CH}_2\text{CH}_2\text{O})_5\text{H}$ R = $\text{C}_8\text{H}_{17}$ , fatty alcohol	$1000 \pm 3\%$
Lutensol AN 7	$\text{RO}(\text{CH}_2\text{CH}_2\text{O})_7\text{H}$ R = $\text{C}_{12}\text{C}_{14}$ , fatty alcohol	$900 \pm 5\%$
Lutensol AT 11	$\text{RO}(\text{CH}_2\text{CH}_2\text{O})_{11}\text{H}$ R = $\text{C}_{16}\text{C}_{18}$ , fatty alcohol	$800 \pm 5\%$
Pluronic PE 4300	$\text{HO}(\text{CH}_2\text{CH}_2\text{O})_x(\text{CH}(\text{CH}_3)\text{CH}_2\text{O})_y(\text{CH}_2\text{CHO})_z\text{H}$ Molar mass: 1750 g/mol PPO = 30%	$600 \pm 20\%$
Pluronic PE 6400	$\text{HO}(\text{CH}_2\text{CH}_2\text{O})_x(\text{CH}(\text{CH}_3)\text{CH}_2\text{O})_y(\text{CH}_2\text{CHO})_z\text{H}$ Molar mass: 2900 g/mol PPO = 40%	600–1300

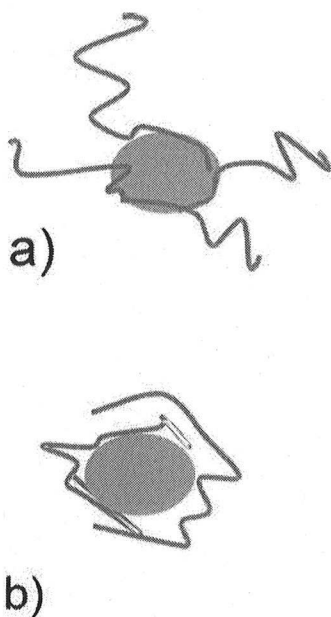


**Figure 3.** Stabilization of primary particles (a) by Lutensol and (b) by Pluronic. (View this art in color at [www.dekker.com](http://www.dekker.com).)

colloids obtained increases with decreasing length of the hydrophobic part (Table 2), as expected from the increasing stabilization of the primary particles by a surfactant with long hydrophobic chains. The length of the hydrophilic part, on the other hand, has no effect on the particles size. This part can be assumed to lie closely on the primary particle surface such that it exerts no significant effect on particle stabilization.

The stabilization by Pluronic polymers is not so effective. It results in a broad size distribution of the titania particles. The average size of the particles can be increased with increasing length of the Pluronic polymer.

In order to determine, whether the polymer is built into the colloidal particles during the aggregation process, we carried out EDX measurements and XRD. The EDX measurements of the colloidal particles show that these particles contain around 7% carbon that stems from the polymer. This result was corroborated by XRD with both electrostatically and sterically stabilized colloids heated up to 400°C (anatase phase). Two typical diffraction patterns are shown in Fig. 4. In the case of electrostatic stabilization, the width of the Bragg peaks is narrow corresponding to larger nanoparticles and in the case of steric stabilization the width is broad corresponding to very small nanoparticles. This indicates that electrostatically stabilized nanoparticles can grow together during the sintering process and that in case of steric stabilization, the polymer around

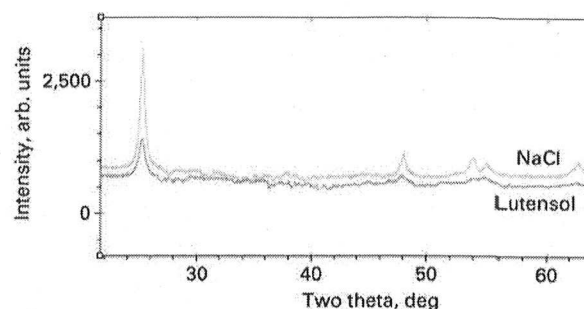


**Figure 4.** XRD pattern of anatase colloidal particles which were obtained by steric and electrostatic stabilization. (View this art in color at [www.dekker.com](http://www.dekker.com).)

the primary particles prevents the formation of larger particles. Therefore, we assume that the polymer is built into the final particles during the aggregation process (Fig. 5). This aggregation model suggests that at the end of the reaction, the particles are porous and the porosity can be controlled by the polymer type. Nitrogen absorption measurements show indeed that the specific surface area ( $a_s$ ), determined by the Brunauer Emmett Teller method, increases when the polymer is added to the reaction medium (Table 3). Lutensol ON 50 yields the largest porosity with  $a_s = 300 \text{ m}^2/\text{g}$ , presumably, because it requires the largest space around the particles and prevents the formation of compact particles. In contrast, the Pluronic polymer stabilizes the primary particles in such a way that the primary particles form more compact aggregates and  $a_s$  decreases to  $200 \text{ m}^2/\text{g}$ . As the electrostatically stabilized colloids are formed without polymer, no porosity is expected and, indeed, the surface area decreases to  $35 \text{ m}^2/\text{g}$ .

In some cases, where hollow or porous titania beads (Fig. 6) were synthesized the porosity can be observed by SEM. To determine whether all colloid particles are hollow, they were heated up to 1000°C. At this temperature, the particles broke to nanoparticles which is the expected behavior for hollow titania beads.<sup>[18]</sup> As no carbon is found in the samples with EDX or elemental analysis and since the pores are much larger than the micelles formed by these polymers,<sup>[19]</sup> we believe that the cause for the formation of these hollow particles is not only the polymer but also the tiny air bubbles that are stabilized by the polymer. When the pressure above the solution was reduced, air bubbles could be observed by eye and less porous and smaller particles were formed. The air bubbles, together with the polymer, might act as seeds on which the titania nanoparticles grow into either hollow beads or porous particles.<sup>[20]</sup> Similar conclusions were reached by Rudloff et al.<sup>[24,25]</sup>

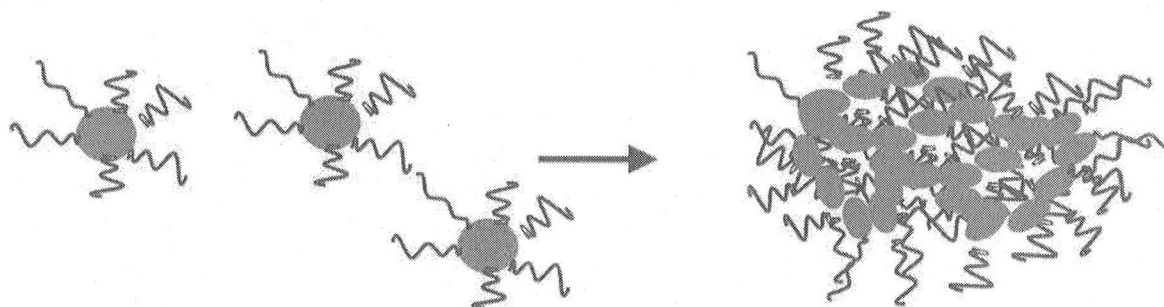


Figure 5. Aggregation mechanism of sterically stabilized primary particles. (View this art in color at [www.dekker.com](http://www.dekker.com).)

for the crystallization of  $\text{CaCO}_3$  in the presence of  $\text{CO}_2$  bubbles and polymer. A more detailed study of this aspect of the formation process is in progress.

#### Structure Determination

The XRD pattern shows that the  $\text{TiO}_2$  phase thus obtained is amorphous. Thermal analysis,  $^1\text{H}$ -MAS-NMR, and x-ray absorption spectroscopy were carried out to determine the local structure. Thermal analysis (Fig. 7) clearly demonstrates the release of one water molecule per unit cell, the amorphous phase thus contains water molecules and/or hydroxide ions. The DTA measurements show three peaks, the first one at about  $250^\circ\text{C}$  and the second one at  $450^\circ\text{C}$  correspond to the release of water, while the third one at  $480^\circ\text{C}$  indicates a phase transition to anatase. For the phase transition to rutile, no DTA peak can be observed, since this phase transition runs from  $600^\circ\text{C}$  to  $1000^\circ\text{C}$ . The presence of hydroxide was evident from the analysis of  $^1\text{H}$ -MAS-NMR spectra (Fig. 8) which clearly show three signals. The line at 1.3 ppm corresponds to hydrogen atoms of terminal Ti OH and the signals at 3.8 and 6.1 ppm correspond to differently bonded water species.

**Table 3.** Specific surface area of titania particles depending on the addition of salt or polymer solution under following conditions: reaction time, 150 min; 100 mL EtOH; 1.50 mL  $\text{Ti}(\text{OEt})_4$ ; 0.50 mL of 0.1 M salt or polymer solution.

Salt solution 0.1 M	Specific surface area ( $\text{m}^2/\text{g}$ )
NaCl	95
$\text{KNO}_3$	35
Lutensol ON 50	300
Lutensol ON 50 in vacuum	130
Pluronic PE 6400	200

Consequently, the analytical techniques suggest that the idealized chemical compositions of the  $\text{TiO}_2$  beads are close to  $\text{TiO}_{1.8}(\text{OH})_{0.4} \cdot 0.8(\text{H}_2\text{O})$  when formed in the presence of salt and to  $\text{TiO}_{1.9}(\text{OH})_{0.2} \cdot 0.9(\text{H}_2\text{O})$  by the addition of polymer. These results show that more hydroxide groups are associated with the

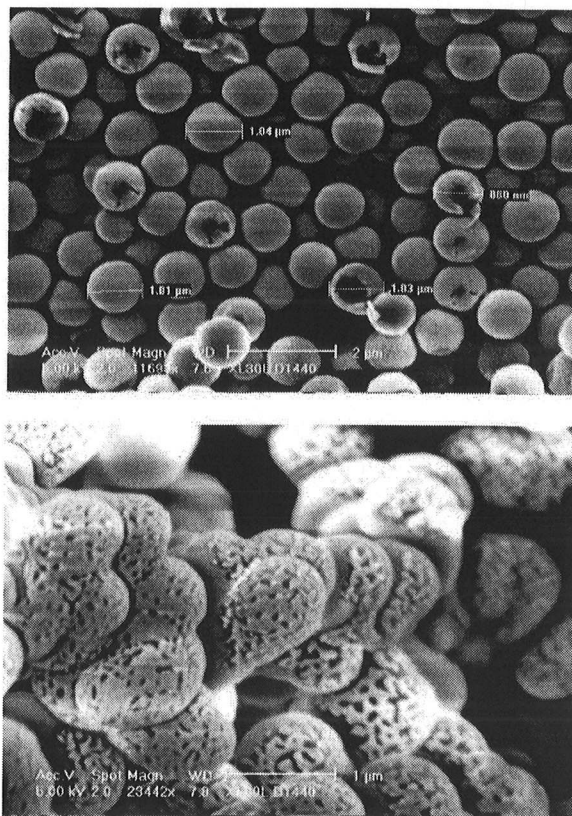
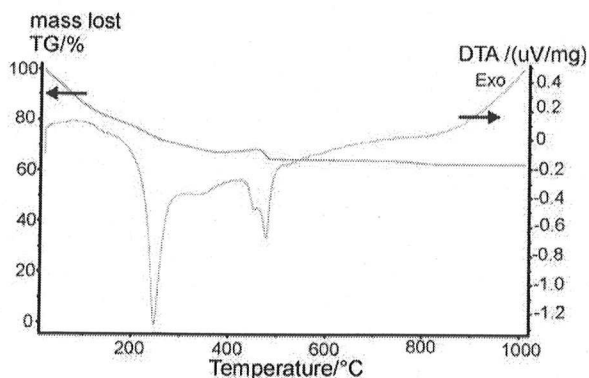
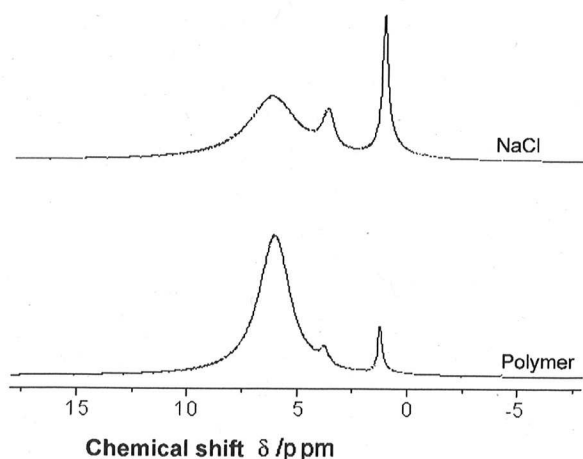


Figure 6. SEM pictures of hollow titania particles produced by addition of Pluronic PE 6400 and porous titania particles produced by addition of Lutensol ON 50.



**Figure 7.** Thermoanalysis of the amorphous titania beads. (View this art in color at [www.dekker.com](http://www.dekker.com).)

electrostatic stabilization than with steric stabilization. In order to investigate the amorphous structure of the hydrous titania phase, x-ray absorption near edge spectroscopy (XANES) was carried out. The spectra (Fig. 9) of titania compounds show different pre-edge peaks that are ascribed to the  $1s \rightarrow 3d$  transition of the excited electron and contain information about the coordination of the Ti atom.<sup>[21]</sup> Compounds with tetrahedrally coordinated Ti show strong absorption. Octahedral coordination results in less pronounced features, up to three peaks may be observed. With increasing distortion, the central peak gains intensity. The pre-edge peak of the titania beads obtained by addition of salt corresponds to very distorted octahedrally coordinated Ti and the pre-edge peak of titania particles obtained by addition of polymer



**Figure 8.**  $^1\text{H}$  MAS NMR measurements of titania particles obtained by addition of salt and polymer.

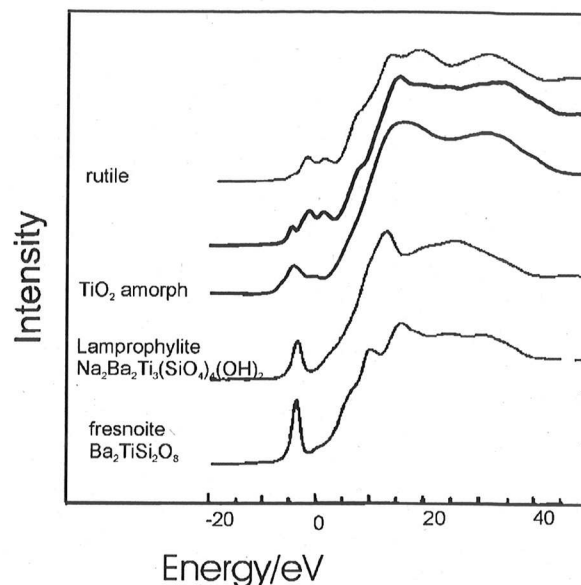


**Figure 9.** Normalized Ti K XANES spectra of the amorphous Titania particles and three reference compounds, rutile, lamprophylite, and fresnoite.

corresponds to octahedrally coordinated Ti. These results indicate that the polymer do not only effect the formation mechanism of the particles but also the structure. The plot of the Fourier transformed EXAFS function shows only one high peak corresponding to a Ti O distance, the second peak corresponding to a Ti Ti distance is very small. This indicates that the amorphous structure is highly disordered. Since the compound is unordered and contains water, it is similar to a gel. Imhof<sup>[22]</sup> reported that his hollow titania particles are deformed after removal of the polystyrene beads, on which they have been grown. This indicates that the structure is very flexible.

#### Hollow Titania Particles

The characteristics of the hollow titania particles obtained from different coating procedures are summarized in Table 4. To determine the optimum conditions for the coating of polystyrene with  $\text{TiO}_2$ , several parameters were varied systematically, including the concentration of reactant and reaction time. It is quite evident that the coating depended strongly on the concentration of  $\text{Ti}(\text{OEt})_4$  in the reaction solution as well as on reaction time. When the  $\text{Ti}(\text{OEt})_4$  was in excess,

**Table 4.** Properties of spherical coated particles obtained by aging ethanolic dispersions containing PS and titanium tetraethoxide.

Sample	PS (g/10mL)	Ti(OEt) <sub>4</sub> (mL/10 mL)	Coated particle diameter (nm)	Thickness of the coat	Reaction time (hr)	System characterization
TLK17c	250	0.3	733	36.5	6	S
TLK17e	250	0.3	830	85	24	R
TLK17i	250	0.3	900	120	31	R
TLK12	250	0.3	830	85	24	S
TLK13	250	0.2	850	95	24	R
TLK14	250	0.3	870	105	24	S
TLK15	250	0.4	900	120	24	S
TLK16	238	0.5	900	120	24	S

Note: S, smooth coated beads; R, rough coated beads; M, mixed systems consisting of coated particles and separated titania particles.

separate titania particles were generated besides the coated particles.

The thickness of the coating layer could be altered by the concentration of Ti(OEt)<sub>4</sub> and the reaction time. When the solvent evaporated completely or the solvent was not stirred permanently aggregated coated powders were obtained. Voids are obtained by complete thermal decomposition in oxygen of polystyrene cores within the coated beads. The calcination was performed at 600°C under oxygen atmosphere. The REM (Fig. 10) of the products shows only hollow titania spheres. In

some of them, openings in the surface was observed. Probably the openings were for the decomposition of the polystyrene beads. The voids were 25–30% smaller than the diameters of the original latex beads, indicating a shrinkage during the sintering process. A series of experiments has shown that the thickness of the TiO<sub>2</sub> coating is an important factor for the stability of the hollow spheres. When the coat was too thin, the hollow spheres were partially burst. The optimum thickness of the coat was found to be in the range of 30–100 nm.

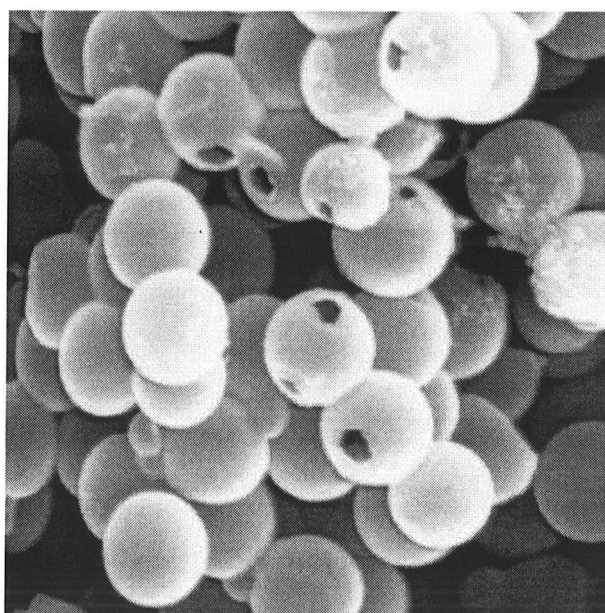


**Figure 10.** REM of hollow beads obtained by calcination the coated particles at 600°C under O<sub>2</sub> atmosphere.

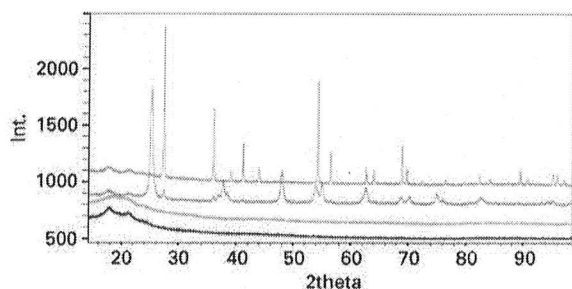


**Figure 11.** X ray diffraction patterns of polystyrene beads, the coated particles and of the same calcinated at 600°C and 1000°C. (View this art in color at [www.dekker.com](http://www.dekker.com).)

The XRD patterns in Fig. 11 show the  $\text{TiO}_2$  phases formed at different temperature. After the coating process, the titania phase obtained is amorphous. When the coated particles were calcined at 600°C anatase type of  $\text{TiO}_2$  with a small part of rutile were obtained. However, calcination at 1000°C yielded  $\text{TiO}_2$  particles consisting exclusively of rutile. The width of the Bragg peaks decrease during the sintering process indicating that the titania nanoparticles forming the coat grow together during this process. The SEM [Fig. 12(a) and (b)] shows nanoparticles and in some cases hollow rutile spheres. The relations between the reaction conditions and the products are shown in Table 5. When the diameter of the polystyrene beads was larger than 900 nm, hollow rutile spheres were obtained. In the other case nanoparticles were created. Possibly, when the diameter of the polystyrene beads is smaller, the curvature of the coat is probably too high for the formation of a stable rutile coat consisting of larger nanoparticles than in the case of anatase, so that a strain was built up and the hollow spheres were broken to nanoparticles. These results are in a good agreement with those of Shiho and Kawahashi.<sup>[23]</sup> They described that their hollow anatase spheres having a diameter of 480 nm burst in nanoparticles at 900°C, too.

## CONCLUSION

We have shown that the size, the porosity, and the monodispersity of colloidal titania particles can be controlled by careful choice of surfactants and of salts added during the synthesis. We obtained particles with narrow size distribution from 50 nm to 2500 nm in diameter of variable porosity. In particular,

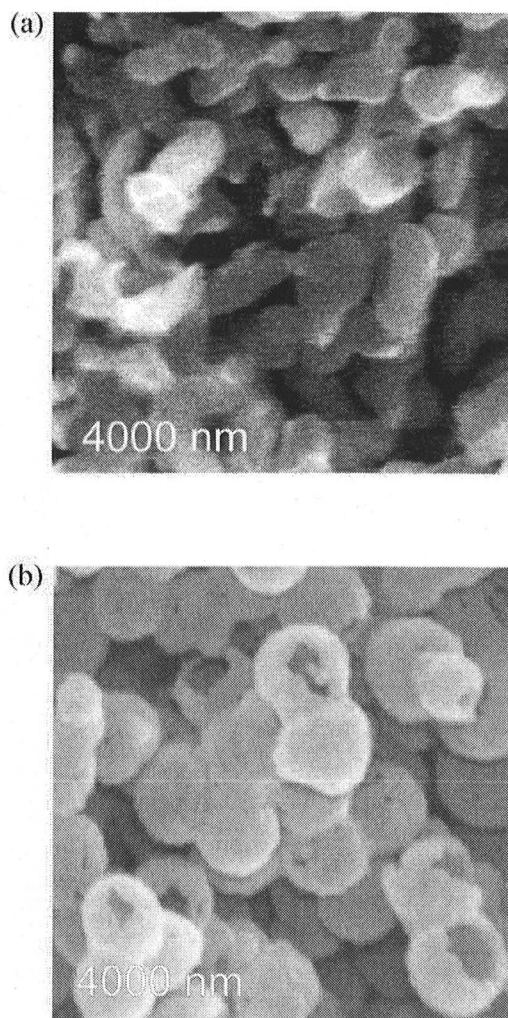


**Figure 12.** (a) REM of particles obtained at 1000°C whose polystyrene core was smaller than 900 nm and (b) REM of particles whose polystyrene core was larger than 900 nm.

we have synthesized very monodisperse titania particles with diameters of 800, 900, and 1000 nm in a reproducible way by using the diblock-copolymer Lutensol.

Furthermore, we present a novel and simple synthesis of hollow rutile beads. The voids of these hollow spheres were determined by the diameter of the polystyrene template and the thickness of the ceramic wall could easily be tailored in the range of 10–100 nm by using precursor solutions with different concentrations.

Depending on the maximum calcination temperature, the  $\text{TiO}_2$  shell of the hollow beads was either

**Table 5.** The influence of the size of the polystyrene beads on the hollow beads.

Sample	Diameter of the polystyrene spheres	Thickness of the TiO <sub>2</sub> coat	Anatase hollow sphere	Rutile hollow sphere
TL1	1,300 nm	40 nm	++	+
TL2	1,100 nm	30 nm	++	+
TL11	888 nm	25 nm	+	
TL12	888 nm	45 nm	++	+
TL13	888 nm	20 nm	+	
TL19	800 nm	100 nm	++	
TL20	555 nm	40 nm	+	
TL21	611 nm	10 nm		
TLK1	527 nm	50 nm	++	

*Note:* ++, perfect hollow spheres; +, hollow spheres with many openings in the surface; , no hollow spheres.

anatase or rutile. Polystyrene beads larger than 900 nm yielded the desired hollow rutile beads.

#### ACKNOWLEDGMENTS

The authors gratefully acknowledge the help of M. Hartl (University of Hannover) for the EXAFS measurements, M. Piech (University of Yale) for the AFM picture and Dr. habil. H. Koller (University of Münster) for the <sup>1</sup>H-MAS-NMR measurements. We kindly acknowledge access to characterization techniques in the groups of Prof. Felsche, Prof. Scheer, Prof. Leiderer, and Prof. Rathmayer. This work was performed by the financial support from the Deutsche Forschungsgemeinschaft (SPP 1113, MA 817/5-3 University of Konstanz).

#### REFERENCES

- Vlachopoulos, N.; Liska, P.; Augustynski, J.; Grätzel, M. Very efficient visible light energy harvesting and conversion by spectral sensitization of high surface area polycrystalline titanium dioxide films. *J. Am. Chem. Soc.* **1998**, *110*, 1216–1220.
- Birner, A.; Busch, K.; Müller, F. Photonische Kristalle. *Physikalische Blätter* **1999**, *55*, 27–33.
- Ohmori, M.; Matijevec, E. Letter to the editor preparation and properties of uniform coated colloidal particles. VII. Silica on hematite. *J. Colloid Interf. Sci.* **1992**, *150*, 594–598.
- Hsu, W.P.; Yu, R.; Matijevec, E. Paper whiteners: I. Titania coated silica. *J. Colloid Interf. Sci.* **1993**, *156*, 56–65.
- Matijevec, E.; Budnik, M.; Meites, L. Preparation and mechanism of formation of titanium dioxide hydrosols of narrow size distribution. *J. Colloid Interf. Sci.* **1977**, *61*, 302–311.
- Jean, J.H.; Ring, T.A. Nucleation and growth of monosized TiO<sub>2</sub> powders from alcohol solution. *Langmuir* **1986**, *2*, 251–255.
- Barringer, E.A.; Bowen, H.K. Formation, packing, and sintering of monodisperse TiO<sub>2</sub> powders. *Commun. Am. Ceram. Soc.* **1982**, *65*, 199–201.
- Edelson, L.H.; Glaeser, A.M. Role of particle substructure in the sintering of monosized titania. *J. Am. Ceram. Soc.* **1988**, *71*, 225–235.
- Look, J.-L.; Zukoski, C.F. Shear induced aggregation during the precipitation of titanium alkoxides. *J. Colloid Interf. Sci.* **1992**, *153*, 461–482.
- Look, J.-L.; Bogush, G.H.; Zukoski, C.F. Colloidal interactions during the precipitation of uniform sub-micrometre particles. *Faraday Discuss. Chem. Soc.* **1990**, *90*, 345–357.
- Zukoski, C.F.; Chow, M.K.; Bogush, G.H.; Look, J.-L. Precipitation of uniform particles: the role of aggregation. *Mater. Res. Soc. Symp.* **1990**, *180*, 131–140.
- Zhong, Z.; Yin, Y.; Gates, B.; Xia, Y. Preparation of mesoscale hollow spheres of TiO<sub>2</sub> and SnO<sub>2</sub> by templating against crystalline arrays of polystyrene beads. *Adv. Mater.* **2000**, *12*, 206–209.
- Rengarajan, R.; Jiang, P.; Colvin, V.; Mittleman, D. Optical properties of a photonic crystal of hollow spherical shells. *Appl. Phys. Lett.* **2000**, *77*, 3517–3519.
- Furusawa, K.; Norde, W.; Lyklema, J. A method for preparing surfactant-free polystyrene lattices of high

- surface charge. *J. Kolloid Z.Z. Polym.* **1972**, *250*, 908.
16. Bogush, G.H.; Zukoski, C.F. Studies of the kinetics of precipitation of uniform silica particles through the hydrolysis and condensation of silicon alkoxides. *J. Colloid Interf. Sci.* **1991**, *142*, 1–18.
  17. LaMer, V.K.; Dinegar, R.H. Theory, production and mechanism of formation of monodispersed hydrosols. *J. Am. Chem. Soc.* **1950**, *72*, 4847–4851.
  18. Eiden, S.; Maret, G. Synthesis and characterization of rutile beads. *J. Colloid Interf. Sci.* **2002**, *250*, 281–284.
  19. Jang, J.; Ha, H. Fabrication of hollow polystyrene nanospheres in microemulsion polymerization using triblock copolymers. *Langmuir* **2002**, *18*, 5613–5618.
  20. Privman, V.; Goiy, D.V.; Park, J.; Matijevic, E. Mechanism of formation of monodispersed colloids by aggregation of nanosize precursors. *J. Colloid Interf. Sci.* **1999**, *213*, 36–45.
  21. Behrens, P.; Felsche, J.; Vetter, S.; Schulz-Ekloff, G.; Jaeger, N.I.; Niemann, W. A XANES and EXAFS investigations of titanium silicalite. *J. Chem. Soc. Commun.* **1991**, 678–680.
  22. Imhof, A. Preparation and characterization of titania coated polystyrene spheres and hollow titania shells. *Langmuir* **2001**, *17*, 3579–3585.
  23. Shiho, H.; Kawahashi, N. Titanium compounds as coatings on polystyrene latices and as hollow beads. *Colloid Polym. Sci.* **2000**, *278*, 270–274.
  24. Rudloff, J.; Antonietti, M.; Cölfen, H.; Pretula, J.; Kaluzynski, K.; Penczek, S. Double-hydrophilic block polymers with monophosphate ester moieties as crystal growth modifiers of CaCO<sub>3</sub>. *Macromol. Chem. Phys.* **2002**, *203*, 627–635.
  25. Rudloff, J. Doppelhydrophile blockpolymere: Synthese und einatz in der biomimetischen morphosynthese von CaCO<sub>3</sub>. Potsdam, 2001; Ph.D. Thesis.